In vivo imaging of antileukemic drug asparaginase reveals a rapid macrophage mediated clearance from the bone marrow

Laurens T van der Meer[1]*, Samantha YA Terry[2,3]*, Dorette S van Ingen Schenau[1], Kiki C Andree[1], Gerben M Franssen[2], Debbie M Roeleveld[1,4], Josbert M Metselaar[5], Thomas Reinheckel[6,7,8], Peter M Hoogerbrugge[9], Otto C Boerman[2], Frank N van Leeuwen[1]

[1]Laboratory of Pediatric Oncology, Radboud Insititute for Molecular Life Sciences, Radboud university medical center, Nijmegen, the Netherlands [2] Department of Radiology and Nuclear Medicine, Radboud university medical center, Nijmegen, the Netherlands [3]Department of Imaging Chemistry and Biology, Division of Imaging Sciences and Biomedical Engineering, King's College London, London, United Kingdom [4]Experimental Rheumatology, Radboud Insititute for Molecular Life Sciences, Radboud university medical center, Nijmegen, the Netherlands [5]Department of Experimental Molecular Imaging, University Clinic and Helmholtz Institute for Biomedical Engineering, RWTH-Aachen University, Aachen, Germany [6]Institute of Molecular Medicine and Cell Research, Albert-Ludwigs-University, Freiburg, Germany [7]German Cancer Consortium (DKTK), Freiburg, Germany [8]BIOSS Centre for Biological Signalling Studies, Albert-Ludwigs-University, Freiburg, Germany [9]Princess Maxima Center for Pediatric Oncology, Utrecht, the Netherlands

* L.T.v.d.M. and S.Y.A.T. contributed equally to this study

Running title

Imaging of asparaginase biodistribution

Keywords

Leukemia, asparaginase, imaging, macrophages, cathepsin B

First Author

Laurens van der Meer

412 Laboratory of Pediatric Oncology,

Radboud university medical center, PO Box 9101,

6500 HB Nijmegen, The Netherlands

+31 (0) 243666203

Laurens.vandermeer@radboudumc.nl

Corresponding Author

Frank N. van Leeuwen

412 Laboratory of Pediatric Oncology,

Radboud university medical center, PO Box 9101,

6500 HB Nijmegen, The Netherlands

+31 (0) 243666203

FrankN.vanleeuwen@radboudumc.nl

3

Conflict of interest disclosure

The authors have no relevant conflict of interest to declare.

Word count: 4822

Figure count: 4 figures, 5 supplemental figures

ABSTRACT

The antileukemic drug asparaginase, a key component in the treatment of acute lymphoblastic leukemia, acts by depleting asparagine from the blood. However, little is known about its pharmacokinetics and mechanisms of therapy resistance are poorly understood. Here, we explored the in vivo biodistribution of radiolabeled asparaginase, using a combination of imaging and biochemical techniques, and provide evidence for tissue specific clearance mechanisms, which could reduce effectiveness of the drug at these specific sites.

Materials and methods: In vivo localization of Indium-111-labeled *E.coli* asparaginase was carried out in C57Bl/6 mice by both micro Single Photon Emission Computed Tomography / Computed Tomography (microSPECT/CT) and by ex vivo biodistribution studies. Mice were treated with liposomal clodronate to investigate the effect of macrophage depletion on tracer localization and drug clearance in vivo. Moreover, macrophage cell line models RAW264.7 and THP-1, as well as knockout mice, were used to identify the cellular and molecular components controlling asparaginase pharmacokinetics.

Results: In vivo imaging and biodistribution studies showed a rapid accumulation of asparaginase in macrophage-rich tissues such as liver, spleen and in particular bone marrow. Clodronate-mediated depletion of phagocytic cells markedly prolonged the serum half-life of asparaginase in vivo and decreased drug uptake in these macrophage rich organs. Immunohistochemistry and in vitro binding assays confirmed the involvement of macrophage-like cells in the uptake of asparaginase. We identified the activity of the lysosomal protease cathepsin B in macrophages as a rate-limiting factor in degrading asparaginase both in vitro and in vivo.

Conclusion: We show that asparaginase is rapidly cleared from the serum by liver, spleen and bone marrow-resident phagocytic cells. As a consequence of this efficient uptake and protease mediated

degradation, particularly bone marrow resident macrophages may provide a protective niche to leukemic cells.

INTRODUCTION

The therapeutic enzyme asparaginase is an essential component of the multi-drug regimen used in the treatment of children and adults with acute lymphoblastic leukemia (ALL). Upon administration, this drug converts serum asparagine into aspartate, thereby effectively depleting the blood from this amino acid. Unlike most other cells in the body, lymphocytes, including leukemic blasts, are fully dependent on uptake of asparagine from the blood and die as a result of nutrient stress (1).

The effectiveness of asparaginase treatment relies on the complete depletion of asparagine from the leukemic cell niche. It has been suggested that during asparaginase treatment, leukemic cell survival is supported by asparagine released by surrounding mesenchymal cells (2,3). Although asparagine levels are significantly higher in bone marrow aspirates when compared to matched blood samples, these levels drop upon treatment with asparaginase (4,5). However, analyses of aspirates may not accurately reflect asparagine concentrations in situ.

Despite the fact that asparaginase has been a cornerstone of ALL treatment protocols since its introduction in the 1970s, little is known about the fate of the infused asparaginase and the mechanisms that determine the pharmacodynamics of this drug. With a molecular weight of 170 kDa that greatly exceeds the limits for renal filtration (~60 kDa), mononuclear phagocyte system (MPS) (or reticulo-endothelial) based clearance is the suggested mode of degradation (6).

Furthermore, the intracellular/molecular mechanisms that influence asparaginase pharmacokinetics remain poorly understood. One study showed that the lysosomal cysteine proteases legumain (or Asparagine Endopeptidase) and cathepsin B efficiently degrade asparaginase in vitro (7). Consistent with these observations, we recently identified a patient carrying a germline mutation in cathepsin B who showed strongly delayed asparaginase degradation (8). However, further validation of these findings and their clinical implications is needed.

6

In the present study we used microSPECT/CT imaging to visualize the in vivo distribution of [111]Indium-labeled asparaginase in a mouse model and identified both cellular and molecular components that determine asparaginase pharmacokinetics.

MATERIALS AND METHODS

Full details on all methods and equipment are presented in the supplemental materials available online.

Mouse models

All animal experiments were approved by the Animal Experimental Committee of the Radboud university medical center and performed in accordance with institutional and national guidelines. Wildtype C57Bl/6J mice were obtained from Charles River (Leiden, the Netherlands). Cathepsin B knockout mice were described previously (9) and have been backcrossed to C57Bl/6J for 10 generations. All mice were housed in individually ventilated filter-top cages, and a standard diet and water were provided ad libitum. The mice were used between ages 8 and 10 weeks.

Micro-SPECT/CT imaging

Mice were injected intravenously with 3 I.U. / gram of bodyweight of ^{111}In-DTPA-asparaginase (21-24 MBq/mouse in 200 µL, see supplemental methods for labeling procedure) and scanned under anesthesia (isoflurane/O_2) at indicated time points after injection using the U-SPECT-II/CT ((MILabs, Utrecht, the Netherlands (10)). CT scans (spatial resolution 160 µm, 65 kV, 615 µA) were acquired for anatomical reference. SPECT scans, (3 frames of 17 min), were reconstructed using an ordered-subset expectation maximization algorithm, with a voxel size of 0.4 mm. SPECT images were analyzed quantitatively as described previously (11).

Biodistribution experiments

Mice were injected intravenously with 3 I.U. ^{111}In-DTPA-asparaginase / gram of bodyweight. Mice were euthanized by CO_2/O_2 asphyxiation at the indicated times after injection. Blood and major organs

8

and tissues were dissected, weighed, and counted in a gamma counter. In addition, organs were used for autoradiography and immunohistochemical analysis (see supplemental methods for procedures).

Pharmacokinetics experiments

Mice were injected intravenously with 3 I.U. Asparaginase/gram of bodyweight (Takeda, Hoofddorp, the Netherlands). At the indicated times after injection, mice were euthanized by CO_2/O_2 asphyxiation, a blood sample was drawn and tissues of interest were dissected. When indicated, mice were pretreated with 150 µl (1 mg/ml clodronate) liposomes or control liposomes (12) via tail vein injection 24 hours before administration of ^{111}In-labeled asparginase. Residual asparaginase activity in serum was determined by photometric detection of the ammonia release after reaction with Nessler's reagent (Sigma-Aldrich, Gorinchem, the Netherlands). In brief, 15 µl serum was diluted with 60 µl 44 mM L-asparagine (Sigma-Aldrich) dissolved in 15 mM Tris-HCl buffer, pH 7.3, supplemented with 0.015% (w/v) BSA and incubated at 37 °C for 30-45 min. The reaction was stopped by the addition of 50 µl trichloroacetic acid (24.5% (w/v), Sigma-Aldrich). After centrifugation 15 µl of the supernatant was added to 120 µl Nessler's solution diluted with deionized water (1:8). The optical density of the solution was measured at 450 nm using the Multiskan Ascent plate reader (MTX Lab systems, Vienna, VA).

Cathepsin B activity assay

Cathepsin B activity was measured using the fluorescent substrate Ac-RR-AFC according to manufacturer's instructions (BioVision, San Francisco, CA). Prism software was used to plot the data and for statistical analysis. $p < 0.05$ was considered a significant difference.

Asparaginase degradation assay

THP-1 and RAW264.7 cells (see supplemental methods for culture conditions) were lysed by freeze-thawing in degradation buffer (50 mM trisodium citrate buffer, pH 4.5, 5 mM Dithiotreitol), cleared by centrifugation. For each timepoint, 5 I.U./ml asparaginase was incubated in lysate containing

9

20 µg of protein. Where indicated, 1 µM Ca-074 (Sigma-Aldrich) was added to inhibit cathepsin B activity. After incubation, asparaginase activity was determined by photometric detection of the ammonia release after reaction with Nessler's reagent using the Multiskan Ascent plate reader as described above. Prism software was used to plot the data and for statistical analysis. ANOVA was used to test for significance; $p < 0.05$ was considered a significant difference.

shRNA mediated knockdown

For lentiviral transduction, HEK293FT cells were transfected with one lentiviral pLKO.1-puro vector (Dharmacon / GE Healthcare), see Supplemental Table 1 for shRNA sequences) together with pVSV-G and psPAX2 using Lipofectamine 2000 (Invitrogen). THP-1 cells were transduced in the presence of 8µg/mL polybrene and 24 hours after transduction selected with 1µg/mL puromycin (Sigma-Aldrich).

RESULTS

MicroSPECT/CT and biodistribution of Asparaginase

To gain more insight into the in vivo distribution of asparaginase and its degradation, we injected mice with ^{111}In-labeled asparaginase and monitored its biodistribution (Fig. 1, Supplemental Movie 1). Imaging (Fig. 1A) and ex vivo biodistribution (Fig. 1B) data showed similar trends. Two hours after injection, asparaginase was mainly present in the circulation (15.8 ± 1.4 %ID/g). However, already at this time point we observed accumulation in the liver (8.5 ± 0.4 %ID/g) and spleen (21.1 ± 3.6 %ID/g), the organs in which a large part of the phagocytic cells reside that make up the MPS (Fig. 1B). Additionally, we observed that a significant part of radiolabeled asparaginase label rapidly localized to the skeleton (femur at 2 hours post injection: 13.0 ± 4.0 %ID/g), suggesting active uptake by bone marrow resident cells. Over time, the radiolabeled drug levels decreased in the blood pool, but drug uptake in the femur remained stable (at 19 hours post injection: 14.6 ± 1.7 %ID/g) and increased in the spleen (42.1 ± 15.9 %ID/g) and liver (10.5 ± 1.5 %ID/g). (Fig. 1B).

Quantitative SPECT analysis revealed an almost identical in vivo distribution as determined by ex vivo biodistribution (Fig. 1C, Supplemental Fig. 1B). For instance, radiolabeled asparaginase cleared rapidly from the blood and increased in the spleen over time (7.9 ± 1.9 %ID/g and 13.8 ± 3.8 %ID/g at 2 and 19h post injection, respectively). Uptake of ^{111}In-asparaginase in the femur and sternum remained unaltered at 2 (10.1 ± 2.4 %ID/g) and 19h (11.5 ± 2.0 %ID/g) post injection. Quantitative SPECT data and biodistribution data correlated well as shown in figure 1D (Spearman r at 0.7996).

Autoradiography (Supplemental Fig. 2A) and immunohistochemical analysis using anti-asparaginase antibodies (Supplemental Fig. 2B) were used to study asparaginase localization in more detail. This revealed accumulation of asparaginase in the bone marrow in spinal cord and hind legs. Uptake in the spleen was restricted to the macrophage-rich structure known as red pulp. The

11

accumulation of asparaginase in the kidney was limited to the cortex of this organ, consistent with glomerular entrapment. The asparaginase immune stainings showed a similar pattern to that of the macrophage marker F4/80 , suggesting that macrophage-like cells are responsible for the uptake. Together these results point towards a crucial role for phagocytic cells in liver, spleen and bone marrow in the clearance of asparaginase, which is in line with a previous study that showed that asparaginase kinetics are affected by virus mediated inhibition of macrophage function (13).

Macrophage depletion by clodronate liposomes disrupts asparaginase biodistribution

To further study the role of phagocytic cells for asparaginase biodistribution and turnover, we used clodronate liposomes to deplete phagocytic cells from the organs of interest. We observed an almost complete depletion of F4/80 positive macrophages in liver and spleen and a marked decrease of the numbers of macrophages in bone marrow (Supplemental Fig. 3) 24 hours after injection of clodronate liposomes. Clodronate pretreatment significantly prolonged the serum half-life of asparaginase (Fig. 2A). MicroSPECT/CT (Fig. 2B and Supplemental Movie 2) and ex vivo biodistribution assays (Fig. 2C) confirmed that clodronate pre-treatment markedly affected the in vivo distribution of asparaginase. SPECT scans of control mice were similar to those obtained in previous experiments (data not shown). In contrast, in clodronate-treated mice, asparaginase was still detectable in the circulation, while little activity was observed in liver (2.5 ± 0.4 %ID/g) and spleen (3.2 ± 0.5 %ID/g), indicating a near complete block in asparaginase uptake by these organs. Furthermore, accumulation in the bone marrow was significantly diminished (femur: 7.2 ± 4.5 %ID/g; spine: 2.2 ± 0.5 %ID/g; sternum: 2.8 ± 0.9 %ID/g), which is consistent with the partial depletion of macrophages in this tissue (Supplemental Figs. 3e,f). Together our results establish a central role for phagocytic cells in the regulation of asparaginase pharmacokinetics.

Assessment of the biological clearance mechanism

12

Our data indicate highly efficient uptake of asparaginase by murine phagocytic cells. To determine whether these findings could be replicated with human cells, we incubated freshly isolated PBMCs from healthy volunteers with fluorescein isothiocyanate-labeled asparaginase and used flow cytometry to assess which cells bind/internalize asparaginase. Consistent with our observations in mice and with previous reports (13,14), predominantly cells expressing the monocyte/macrophage marker CD14 (76.4 ± 14.8 %) were found to bind asparaginase (Fig. 3B).

In an earlier study, we identified lysosomal protease cathepsin B as a critical determinant of asparaginase half-life (8). In order to link this observation to the potential role for phagocytic cells identified here, we studied the role of cathepsin B in macrophage-mediated degradation of asparaginase. To this end, we used THP-1 cells, a human monocytic cell line that can be forced into differentiation towards a macrophage like phenotype using phorbol-12-myristate-13-acetate. Similar to freshly isolated CD14+ cells, THP-1 cells efficiently bound asparaginase (Supplemental Fig. 4). We used a previously described in vitro degradation assay (8) to show that asparaginase activity remained unaffected in the monocyte lysate, while the protein was rapidly degraded in lysates from differentiated cells. We observed a similar, but even more efficient degradation in lysates of the murine macrophage cell line RAW264.7. Importantly, degradation in both macrophage lysates was completely inhibited by the addition of the cathepsin B inhibitor CA-074 (Fig. 3C, red marked values).

To investigate the correlation between cathepsin B expression and asparaginase degradation, we compared cathepsin B mRNA expression levels in undifferentiated versus differentiated THP-1 cells, (Fig. 4A) and found that cathepsin B mRNA expression is strongly induced upon differentiation. RNAi mediated suppression of cathepsin B activity (Fig. 4B and Supplemental Figs. 5A and B) resulted in a complete or partial block of asparaginase degradation, depending on knockdown efficiency (Fig. 4C). Furthermore, we observed that the serum half-life of asparaginase was strongly prolonged in cathepsin B

13

knockout mice compared (Fig. 4D). Together, these data firmly establish that cathepsin B activity is an

essential and a rate-limiting enzyme for asparaginase degradation by macrophages.

DISCUSSION

Despite the fact that asparaginase has been used for decades in the treatment of patients with ALL, little is known about its metabolic fate in patients. Although depletion of asparagine in serum and bone marrow aspirates can be monitored and shows complete depletion when asparaginase concentrations reach threshold levels, concentrations in situ and the supportive role of the microenvironment are subject of debate (2,3,5,15-18). The question remains whether asparaginase is sufficiently active at this particular niche where the leukemia originates and where leukemia-initiating cells reside.

We applied in vivo imaging of radiolabeled asparaginase with microSPECT/CT to visualize asparaginase biodistribution. In addition to spleen and liver, both organs most frequently involved in uptake of foreign (macro)molecules and particles, we found a remarkably rapid and strong accumulation of asparaginase in the bone marrow (Fig. 1). Although bone marrow resident macrophages are part of the MPS, the role of these cells in clearing the blood from macromolecules is often secondary to spleen and liver resident cells and is directed by the size of the molecule (19,20). Because for its therapeutic action, asparaginase needs to be present in the serum, this raises the question whether rapid clearance of the drug by bone marrow resident macrophages will negatively affect the depletion of asparagine in the bone marrow niche. Hence, our imaging approach may point towards a rapid local elimination of the drug that could provide a mechanism by which leukemic cells can escape from apoptosis as a result of the asparaginase induced nutrient limitation.

We have limited our studies to *E.coli* asparaginase. Two other formulations are in use in clinic practice: *Erwinia chrysamthemi* asparaginase is frequently used as a second line treatment option after development of inhibitory antibodies. In our previous study (8), we showed that the kinetics of *E.coli* and *Erwinia* asparaginase are similarly affected by a mutation in cathepsin B. In addition to its native form, a

15

PEGylated form of *E.coli* asparaginase, which was introduced to reduce hypersensitivity reactions to the drug, is widely used in the clinic. However, recent work indicates that similar to native or recombinant asparaginase, PEG-asparaginase treatment should also be supported by therapeutic drug monitoring to prevent underexposure (21). As a result, the benefits compared to the use of native asparaginase are reduced. Several studies have shown that the structure of asparaginase permits the introduction of modifications without appreciable loss of enzymatic function (7,22,23). The data we present here may provide a rationale for the generation of novel modified versions of asparaginase. Since our data show that phagocytic cells are an important sink for asparaginase, as well as a key determinant of the asparaginase pharmacokinetics, preventing these interactions, by other means than PEGylation, could be of benefit. A modified form of asparaginase that exhibits a reduced affinity for surface receptors of phagocytic cells is expected to have a prolonged half-life, show delayed clearance from the bone marrow and thus enhanced therapeutic efficacy. In addition, since uptake by phagocytic cells and subsequent presentation is the first step in the activation of the immune response, interfering with this initial step may prevent or delay the formation of inhibitory antibodies. Future studies should therefore generate more insight into interaction between these cells and asparaginase.

Only a few studies have addressed the potential molecular mechanisms involved in the regulation of asparaginase kinetics (7,8). We show a highly efficient uptake of asparaginase by phagocytic cells, predominantly macrophages (Figs. 2 and 3). We previously showed that asparaginase is extremely stable when incubated in serum ex vivo (8). Although we cannot exclude that in vivo, asparaginase is subject to degradation in the serum and subsequent endocytosis of fragments, our results point towards active uptake by phagocytic cells. These cells express a large variety of antigen uptake receptors that recognize macromolecules based on charge, peptide structure or modification, which are subsequently internalized and degraded in the endo-lysosomal compartment (24). Previous reports discuss the role of lysosomal proteases in controlling asparaginase degradation in vitro and in

16

vivo (7,8). Our recent finding that the prolonged half-life of asparaginase in a pediatric patient suffering from ALL may be attributed to a germline mutation in the cathepsin B (8), is now further supported by the in vitro and in vivo experiments presented here.

We have shown using both a small-molecule inhibitor and RNAi mediated knockdown (Fig 4) that lysosomal protease cathepsin B is required for the efficient degradation of asparaginase by both human and murine macrophages (Fig. 4). Our in vivo studies demonstrate that loss of cathepsin B leads to a significantly prolonged asparaginase half-life in vivo, while inhibition of cathepsin B activity completely abolishes its degradation in vitro. These results are in accordance with our previous report, which linked a germline loss-of-function mutation in the gene encoding cathepsin B to a prolonged serum half-life of asparaginase in a pediatric patient (8). Based on these results, we conclude that cathepsin B plays a major role the degradation of asparaginase. While the incomplete depletion of phagocytic cells may explain the partial block of asparaginase turnover in the clodronate-treated mice, the fact that cathepsin B knockout mice only display a delayed clearance indicates that other mechanisms of asparaginase will contribute to the regulation of asparaginase kinetics. However, since lysosomal processing of epitopes is a crucial step towards successful antigen presentation, pharmacological inhibition of cathepsin B, which is currently being explored in preclinical setting for a different purpose (25), may not only prolong the serum half-life of the asparaginase, but may also attenuate the immune response directed against this therapeutic protein.

CONCLUSION

By using microSPECT/CT we showed that asparaginase is efficiently cleared by macrophages of the MPS. In particular, bone marrow resident macrophages may provide a protective environment for leukemic cells by effectively removing the therapeutic protein from the bone marrow niche. We conclude that cathepsin B is required for the degradation of asparaginase by macrophages, and that this

degradation aids in the regulation of serum half-life. These new insights into both the prominent role of macrophages and the importance of the lysosomal protease cathepsin B in asparaginase clearance may aid in a rational design of a next generation asparaginase.

REFERENCES

1. Pieters R, Hunger SP, Boos J, et al. L-asparaginase treatment in acute lymphoblastic leukemia: a focus on Erwinia asparaginase. *Cancer.* 2011;117:238-249.

2. Ehsanipour EA, Sheng X, Behan JW, et al. Adipocytes cause leukemia cell resistance to L-asparaginase via release of glutamine. *Cancer Res.* 2013;73:2998-3006.

3. Iwamoto S, Mihara K, Downing JR, Pui CH, Campana D. Mesenchymal cells regulate the response of acute lymphoblastic leukemia cells to asparaginase. *J Clin Invest.* 2007;117:1049-1057.

4. Tong WH, Pieters R, Hop WC, Lanvers-Kaminsky C, Boos J, van der Sluis IM. No evidence of increased asparagine levels in the bone marrow of patients with acute lymphoblastic leukemia during asparaginase therapy. *Pediatr Blood Cancer.* 2013;60:258-261.

5. Steiner M, Hochreiter D, Kasper DC, et al. Asparagine and aspartic acid concentrations in bone marrow versus peripheral blood during Berlin-Frankfurt-Munster-based induction therapy for childhood acute lymphoblastic leukemia. *Leuk Lymphoma.* 2012;53:1682-1687.

6. Brueck M, Koerholz D, Nuernberger W, Juergens H, Goebel U, Wahn V. Elimination of l-asparaginase in children treated for acute lymphoblastic leukemia. *Dev Pharmacol Ther.* 1989;12:200-204.

7. Patel N, Krishnan S, Offman MN, et al. A dyad of lymphoblastic lysosomal cysteine proteases degrades the antileukemic drug L-asparaginase. *J Clin Invest.* 2009;119:1964-1973.

8. van der Meer LT, Waanders E, Levers M, et al. A germ line mutation in cathepsin B points toward a role in asparaginase pharmacokinetics. *Blood.* 2014;124:3027-3029.

9. Halangk W, Lerch MM, Brandt-Nedelev B, et al. Role of cathepsin B in intracellular trypsinogen activation and the onset of acute pancreatitis. *J Clin Invest.* 2000;106:773-781.

10. van der Have F, Vastenhouw B, Ramakers RM, et al. U-SPECT-II: An Ultra-High-Resolution Device for Molecular Small-Animal Imaging. *J Nucl Med.* 2009;50:599-605.

11. Terry SY, Abiraj K, Lok J, et al. Can 111In-RGD2 monitor response to therapy in head and neck tumor xenografts? *J Nucl Med.* 2014;55:1849-1855.

12. Terry SY, Boerman OC, Gerrits D, et al. In-anti-F4/80-A3-1 antibody: a novel tracer to image macrophages. *Eur J Nucl Med Mol Imaging.* 2015;42:1430-1438.

13. Nakayama H, Hayashi T, Salata KF, Notkins AL. Flow cytometry to identify cell types to which enzymes bind. Effect of lactic dehydrogenase virus on enzyme binding. *J Biol Chem.* 1990;265:14355-14357.

14. Mori I, Hayashi T, Kitazima S, Yamamoto H. Binding of asparaginase to mouse monocytes. *Int J Exp Pathol.* 1992;73:585-592.

15. Chiu M, Franchi-Gazzola R, Bussolati O, D'Amico G, Dell'Acqua F, Rizzari C. Asparagine levels in the bone marrow of patients with acute lymphoblastic leukemia during asparaginase therapy. *Pediatr Blood Cancer.* 2013;60:1915.

16. Tiziani S, Kang Y, Harjanto R, et al. Metabolomics of the tumor microenvironment in pediatric acute lymphoblastic leukemia. *PLoS One.* 2013;8:e82859.

17. Dimitriou H, Choulaki C, Perdikogianni C, Stiakaki E, Kalmanti M. Expression levels of ASNS in mesenchymal stromal cells in childhood acute lymphoblastic leukemia. *Int J Hematol.* 2014;99:305-310.

18. Zhang W, Trachootham D, Liu J, et al. Stromal control of cystine metabolism promotes cancer cell survival in chronic lymphocytic leukaemia. *Nat Cell Biol.* 2012;14:276-286.

19. Rennen HJ, Makarewicz J, Oyen WJ, Laverman P, Corstens FH, Boerman OC. The effect of molecular weight on nonspecific accumulation of (99m)T-labeled proteins in inflammatory foci. *Nucl Med Biol.* 2001;28:401-408.

20. Brinkhuis RP, Stojanov K, Laverman P, et al. Size dependent biodistribution and SPECT imaging of (111)In-labeled polymersomes. *Bioconjug Chem.* 2012;23:958-965.

21. Tong WH, Pieters R, Kaspers GJ, et al. A prospective study on drug monitoring of PEGasparaginase and Erwinia asparaginase and asparaginase antibodies in pediatric acute lymphoblastic leukemia. *Blood.* 2014;123:2026-2033.

22. Offman MN, Krol M, Patel N, et al. Rational engineering of L-asparaginase reveals importance of dual activity for cancer cell toxicity. *Blood.* 2011;117:1614-1621.

23. Verma S, Mehta RK, Maiti P, Rohm KH, Sonawane A. Improvement of stability and enzymatic activity by site-directed mutagenesis of E. coli asparaginase II. *Biochim Biophys Acta.* 2014;1844:1219-1230.

24. Aderem A, Underhill DM. Mechanisms of phagocytosis in macrophages. *Annu Rev Immunol.* 1999;17:593-623.

25. Olson OC, Joyce JA. Cysteine cathepsin proteases: regulators of cancer progression and therapeutic response. *Nat Rev Cancer.* 2015;15:712-729.
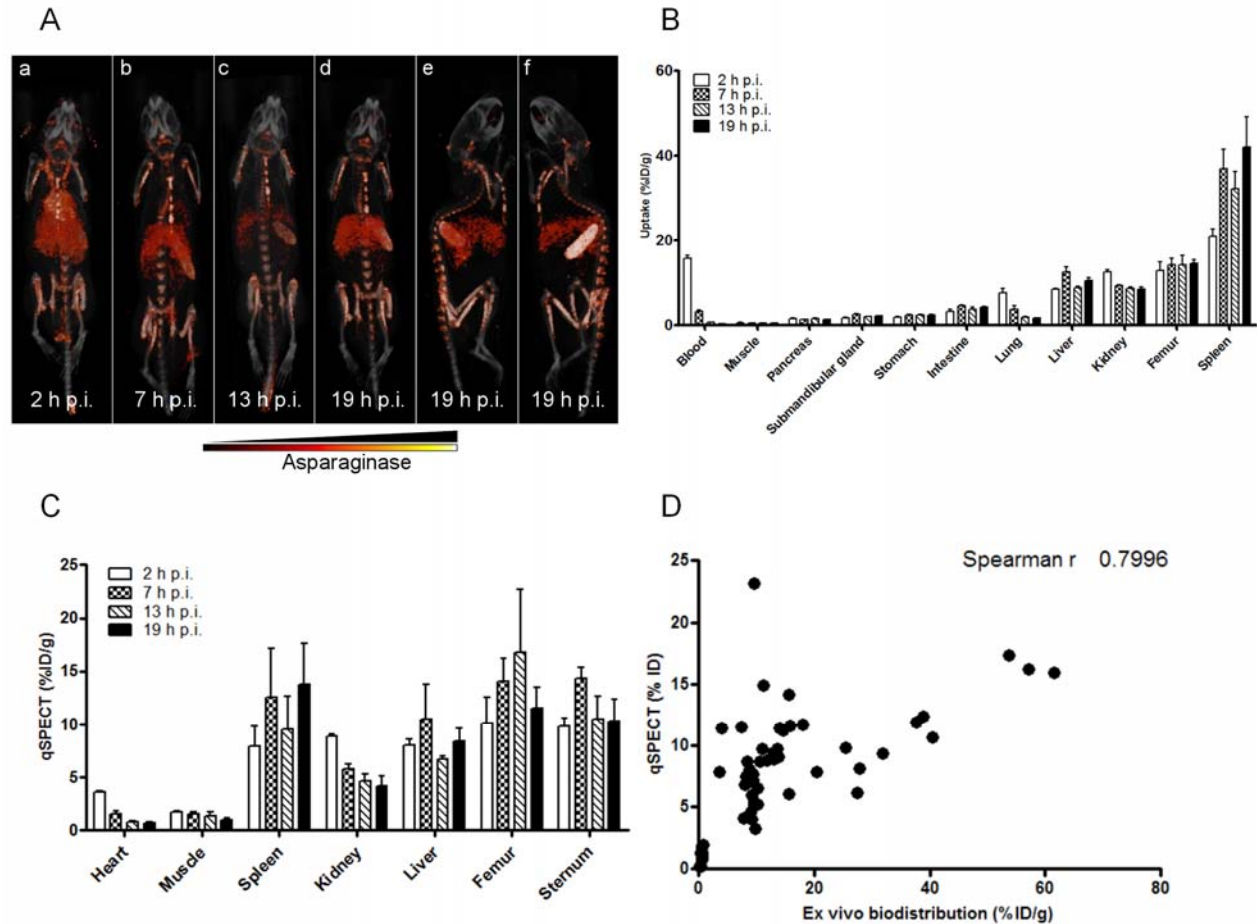
FIGURE LEGENDS

FIGURE 1. Asparaginase rapidly accumulates in spleen, liver and bone marrow

A Ventral (a-d) and lateral (e,f) 3-dimensional volume projections of fused SPECT/CT scans of mice injected with [111]Indium-labeled asparaginase at the indicated hours post injection (h.p.i.).

B Ex vivo quantification of [111]Indium-labeled asparaginase uptake in various organs at the indicated hours post injection (h.p.i.). Data represent mean ± Standard error of the mean (SEM) of n = 5 mice per timepoint.

C Biodistribution of asparaginase as quantified from SPECT images. N=3 per timepoint.

D Uptake of [111]Indium-labeled asparaginase as quantified from micro-SPECT images plotted against values derived from ex vivo biodistribution studies.

21
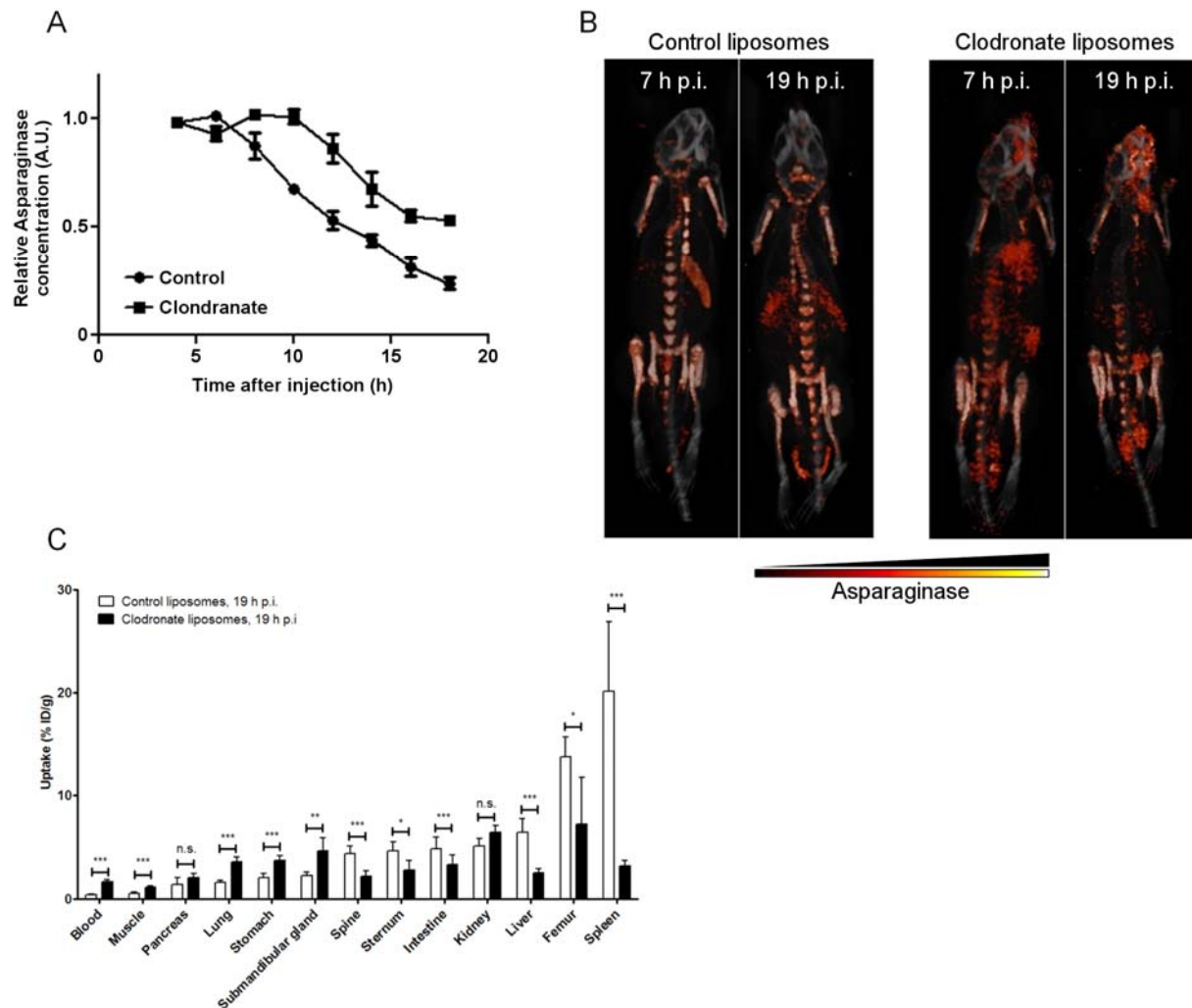
FIGURE 2. Depletion of macrophages affects asparaginase pharmacokinetics and biodistribution

A Residual serum asparaginase activity at the indicated times after injection in mice. Mice were treated with a single dose of control or clodronate liposomes 24 hours prior to the asparaginase injection. At the indicated times after injection of unlabelled asparaginase, serum samples were taken and asparaginase activity was determined as described in the methods section. Data represent mean ± SEM of n = 3 mice per time point per treatment group. ANOVA statistical analysis was applied to test for significance (p<0.05).

B Ventral 3-dimensional volume projections of fused SPECT/CT scans of mice treated with a single dose of control or clodronate liposomes 24 hours prior to the [111]Indium-labeled asparaginase injection. Scans were made at 7 or 19 hours post injection (h p.i) with [111]Indium-labeled asparaginase.

C Ex vivo quantification of [111]Indium-labeled asparaginase uptake in various organs of mice pretreated with control or clodronate liposomes, 19 hours post injection (h p.i.) of asparaginase. Data represent mean ± SEM of n = 5 mice per time point per treatment group. Statistical significance was determined by unpaired two-sided t-test. * = $p < 0.05$, ** = $p < 0.01$, *** = $p < 0.001$.
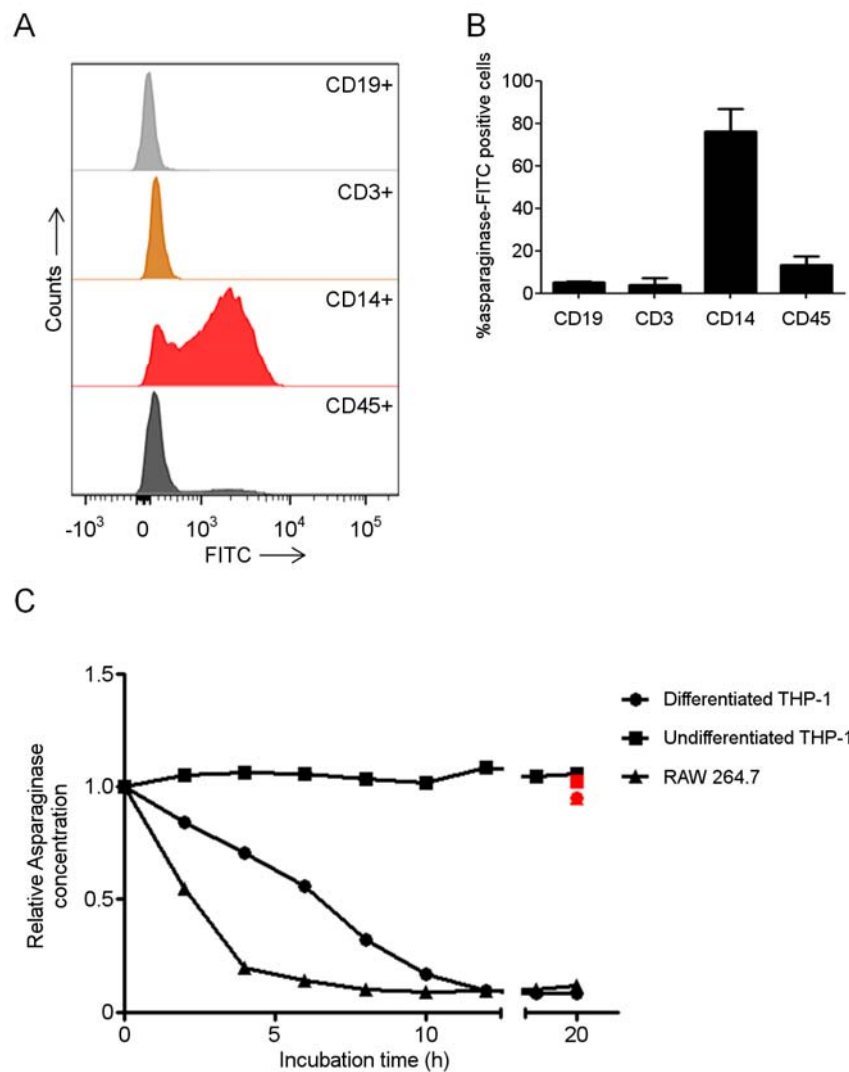
FIGURE 3. Human macrophages bind and degrade asparaginase

A Histograms showing binding of asparaginase to various cellular subsets in PBMCs. Freshly isolated PBMCs were incubated with FITC-labelled asparaginase and subsequently indentified based on the indicated cell surface markers using flowcytometry. Lineages were defined as follows: CD45-all nucleated cells, CD14-monocytes/macrophages, CD3-T cells, CD19-B cells.

B Average of percentage of PBMC subsets binding FITC-labeled asparaginase (N=2).

C Asparaginase degradation in lysates of cell lines. Asparaginase was incubated in lysate of human undifferentiated, monocyte like THP-1 cells (squares), differentiated, macrophage like THP-1 cells

24

(circles) and the murine macrophage cell line RAW264.7 (triangles). After incubation, residual ASNase

activity was assayed as described in the methods section. Cathepsin inhibitor CA-074 was included to

selected samples to confirm the contribution of Cathepsin B in this degradation (red data points).
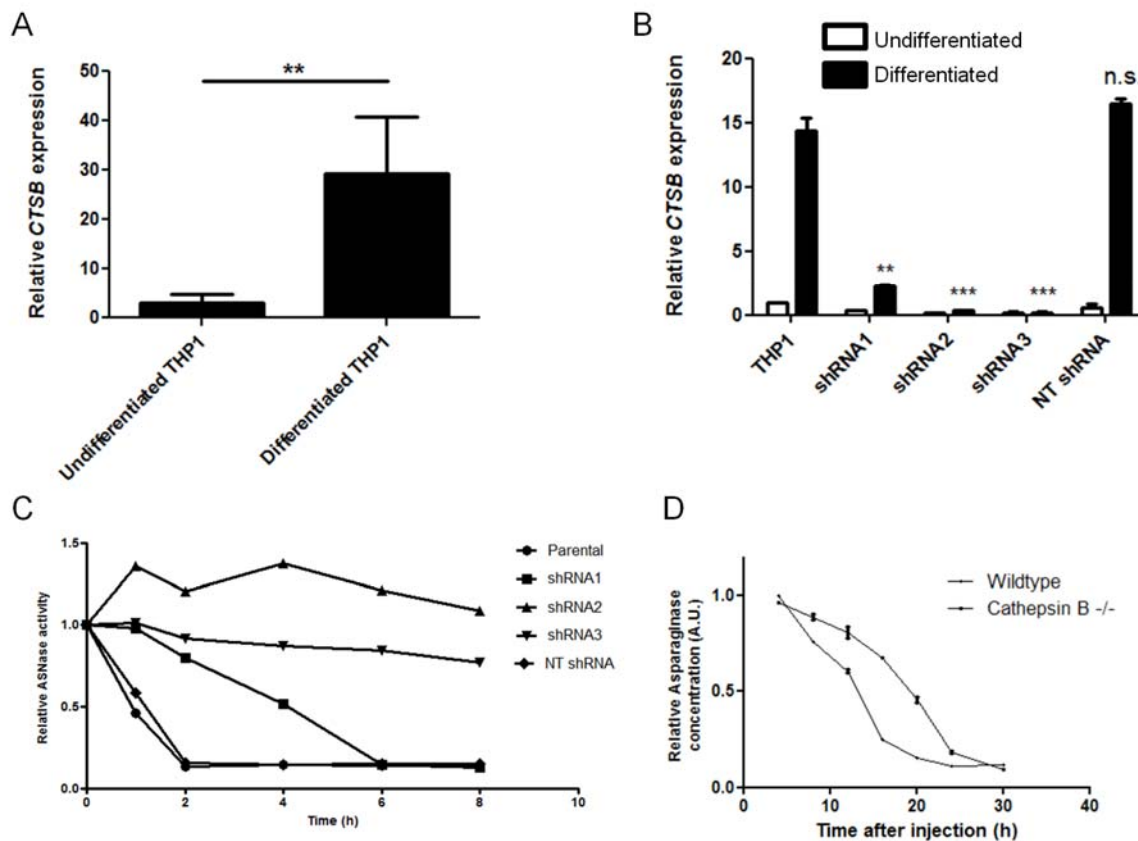
FIGURE 4. Cathepsin B is required for asparaginase degradation and controls asparaginase pharmacokinetics

A Realtime quantitative PCR analysis of Cathepsin B mRNA expression in undifferentiated and PMA induced differentiated THP-1 cells, normalized for expression of TATA binding protein. Data represent mean ± SEM of n = 4. Statistical significance was determined by unpaired two-sided t-test. ** = $p < 0.01$.

B Realtime quantitative PCR analysis of Cathepsin B mRNA expression in undifferentiated and PMA induced differentiated THP-1 cells transduced with shRNAs targeting Cathepsin B or control, non-targeting (NT) shRNA. Data are normalized for TBP expression and shown as mean ± standard deviation of n = 2. Statistical significance was determined by unpaired two-sided t-test. ** = $p < 0.01$.

C Asparaginase degradation in lysates of cell lines. Asparaginase was incubated in lysate of differentiated THP-1 cells, transduced with control of Cathepsin B targeting shRNAs. After incubation, residual ASNase

26

activity was assayed as described in the methods section. A representative example of multiple experiments (N=3) is shown.

D Residual serum asparaginase activity at the indicated times after injection in mice. Cathepsin B knockout mice and age and sex matched control were injected with unlabelled asparaginase. At the indicated times after injection of unlabelled asparaginase, serum samples were taken and asparaginase activity was determined as described in the methods section. Data represent mean ± standard deviation of n = 2 mice per time point per treatment group. ANOVA statistical analysis was applied to test for significance ($p < 0.05$).

The Journal of
NUCLEAR MEDICINE

In vivo imaging of antileukemic drug asparaginase reveals a rapid macrophage mediated clearance from the bone marrow

Laurens T van der Meer, Samantha Y.A. Terry, Dorette van Ingen Schenau, Kiki C Andree, Gerben M Franssen, Debbie M Roeleveld, Bart M Metselaar, Thomas Reinheckel, Peter M Hoogerbrugge, Otto C Boerman and Frank N van Leeuwen

This article and updated information are available at:
http://jnm.snmjournals.org/content/early/2016/08/03/jnumed.116.177741

Information about reproducing figures, tables, or other portions of this article can be found online at:
http://jnm.snmjournals.org/site/misc/permission.xhtml

Information about subscriptions to JNM can be found at:
http://jnm.snmjournals.org/site/subscriptions/online.xhtml

SNMMI | SOCIETY OF NUCLEAR MEDICINE AND MOLECULAR IMAGING